

## Densification Behavior and Mechanical Properties of Niobium-Oxide-Doped Alumina Ceramics

A.M. Hassan<sup>1</sup>, M. Awaad<sup>2</sup>, F. Bondioli<sup>3</sup>, S.M. Naga<sup>\*2</sup>.

<sup>1</sup>Zagazig Uni., Faculty of Engineering, Materials Engineering Dept, 44519 - Zagazig, Egypt

<sup>2</sup>National Research Center, Ceramics Dept, El-Bohous Str., 12622 - Cairo, Egypt

<sup>3</sup>Department of Industrial Engineering, Parco delle Scienze 181/A, 43124 - Parma, Italy

received December 10, 2013; received in revised form January 10, 2014; accepted January 24, 2014

### Abstract

The densification behavior, microstructure and mechanical properties of high-purity  $\alpha$ -Al<sub>2</sub>O<sub>3</sub> doped with 0.25, 0.5 and 0.75 wt% Nb<sub>2</sub>O<sub>5</sub> were investigated. The batches were uniaxially pressed at 220 MPa into discs and rectangular bars and pressureless-sintered at temperature ranging between 1500° and 1650 °C for 1 h. The phase composition of the sintered bodies was followed up with an x-ray diffractometer, while their microstructure was characterized with a scanning electron microscope. The mechanical properties in terms of Vickers hardness (HV1), three-point bending strength and fracture toughness were also measured. The results showed that the addition of Nb<sub>2</sub>O<sub>5</sub> accelerated the densification parameters, reinforced and toughened the obtained bodies. The maximum values for the mechanical properties of the Nb<sub>2</sub>O<sub>5</sub>-doped alumina-based ceramics were 34.4, 35.5 and 29.5 % for bending strength, fracture toughness and Vickers hardness respectively, which are higher than those of the undoped and doped technical alumina.

*Keywords:* Doping, alumina, niobia, microstructure, mechanical properties

### I. Introduction

Alumina has intrinsic characteristics that make it a promising candidate for high-temperature structural and wear-resistant components. However, its poor fracture toughness may limit its use as an advanced engineering material<sup>1-3</sup>.

With the introduction of toughening approaches such as transformation toughening, second-phase reinforcements, grain bridging and others, the bending strength and fracture toughness of alumina-based ceramics have been improved significantly. However, there are still many defects in the whole fabrication process of alumina products. For example, the bridging of metal particles is adverse to the chemical inertness of alumina ceramics, whiskers cannot be dispersed evenly in the ceramic matrix materials, and the effect of transformation toughening decreases as the temperature increases. In addition, these methods are very expensive and reduce the hardness of alumina ceramics. With the emergence of new materials, the toughening additives capable of improving the high-performance alumina-based ceramics have been diversified<sup>4</sup>.

Rare earth elements are not only used in luminescent and magnetic materials but also in engineering ceramics as well. Recent studies have focused on the effects of small amount of additives, dopants or impurities on the behavior of ultrapure alumina. These studies have allowed better understanding of the densification process, microstruc-

tural evolution and mechanical behavior of alumina powders<sup>5,6</sup>. During the synthesis of a ceramic, the microstructural parameters such as grain size and shape are governed by the nature and mobility of the grain boundaries present in the material. Control over these microstructural parameters in alumina is typically achieved with precise control of the processing conditions and the use of dopant elements. It is well established that many dopants such Y, La and Mg routinely added to ceramics exhibit, owing to their larger ionic size, low bulk solubility and a marked tendency to segregate at grain boundaries<sup>7</sup>. On the other hand, Rani *et al.*<sup>6</sup> showed that rare earth element dopants retard the grain growth of alumina. At high temperatures, the rare earth dopants aided microstructural modification and the effect of crack-bridging enhanced the toughness of alumina ceramics.

The presence of segregated dopants at grain boundaries in ceramics could have an effect on mechanical properties such as creep and fracture behavior. This beneficial effect is due to the ability of the RE to inhibit grain boundary diffusion, the primary mechanism for creep in Al<sub>2</sub>O<sub>3</sub>. The RE segregates very strongly at grain boundaries and shows a large (typically two to three orders of magnitude) increase in creep resistance<sup>8</sup>. It has been reported that RE segregates at the Al<sub>2</sub>O<sub>3</sub> grain boundaries either reduce the rate of ion transport along the grain boundaries<sup>9-11</sup> (possibly through the formation of a continuous two-dimensional second phase) or inhibit the interfacial reaction. On the other hand, Rani *et al.*<sup>6</sup> and Deng *et al.*<sup>12</sup> claimed that the substantial increase in the proportion of intergranu-

\* Corresponding author: [salmanaga@yahoo.com](mailto:salmanaga@yahoo.com)

lar fracture of the RE-doped alumina is due to the significant reduction in the free surface energy that results from segregation of the rare earth dopant at grain boundaries, which reduces the required work of fracture for intergranular failure<sup>6,12</sup>.

Acchar and Segades<sup>13</sup> obtained dense alumina-NbC ceramic composites by means of uniaxial hot pressing at 1650 °C. They showed that the addition of 30 wt% NbC increases both the hardness and flexural strength of the alumina matrix by 33.3 % and 20 % respectively. However, the incorporation of NbC into the alumina matrix did not significantly improve the fracture toughness. An Al<sub>2</sub>O<sub>3</sub> ceramic matrix composite toughened with *in-situ* growth TaC whiskers was prepared in two steps. The first is *in-situ* synthesis of TaC whiskers in Al<sub>2</sub>O<sub>3</sub> matrix powder and the second is hot pressing of the composite at 1450 °C. The flexural strength, fracture toughness and Vickers hardness of the composite were 638 MPa, 6.5 MPa m<sup>1/2</sup> and 17.4 GPa respectively<sup>14</sup>. Xihua *et al.*<sup>3</sup> studied the effect of mixed rare earth elements (Nd, Ce La and Pr) on the mechanical properties of alumina ceramics. They showed that the doped ceramics hot pressed in nitrogen atmosphere at 1550 °C exhibited bending strength values between 247.0 and 326.7, Vickers hardness ranging between 17.96 and 18.41 GPa and fracture toughness,  $K_{IC}$ , between 3.52 and 3.69 MPa m<sup>1/2</sup>. The Vickers hardness and fracture toughness of pure alumina specimens depend on the starting material grain size as well as on the preparation method. Chan *et al.*<sup>15</sup> studied the influence of neodymium additions on the densification and microstructure development of alumina at dopant levels of 100, 350, and 1000 ppm. They found that neodymium additions inhibited densification, with a corresponding increase in the apparent activation energy. Anstis *et al.*<sup>16</sup> studied the Vickers hardness and fracture toughness of polycrystalline alumina and they showed that the Vickers hardness of the dense alumina bodies ranged between 13 and 20 GPa, while their fracture toughness,  $K_{IC}$ , ranged from 2.9 to 4.6 MPa m<sup>1/2</sup> depending on the alumina grain size.

The present work mainly analyzes the influence of Nb<sub>2</sub>O<sub>5</sub> doping on the microstructure and mechanical properties of alumina-based ceramics. Different amounts of Nb<sub>2</sub>O<sub>5</sub>, ranging from 0.25 to 0.75 wt%, were added to pure alumina and the effect of the sintering temperature was observed in order to optimize the physical properties (bulk density and apparent porosity) of the materials.

## II. Experimental Procedure

### (1) Materials and processing

Three compositions of 0.25, 0.5 and 0.75 wt% Nb<sub>2</sub>O<sub>5</sub>-doped alumina were prepared by means of powder mixing. The aluminum oxide used had 99.98 % purity (provided by Almatix GmbH Ludwigshafen/RH, Germany), and the niobium oxide had 99.9 % purity (provided by SIGMA-ALDRICH Chemistry, USA). The particle size of the as-received Al<sub>2</sub>O<sub>3</sub> and Nb<sub>2</sub>O<sub>5</sub> ranged from 135 to 150 nm and 100–120 nm respectively. All powders were mechanically mixed in a ball mill for 5 h with 5-mm zirconia balls and a polypropylene container at a constant speed of 300 rpm. The powders obtained were formed by

means of uniaxial pressing at 220 MPa into discs measuring 13 mm in diameter and 4 mm in height (for physical and microstructural characterization) and rectangular bars with the dimensions 6 x 6 x 60 mm<sup>3</sup> (for mechanical evaluation). The bodies formed were pressureless-sintered in an electric oven at a temperature ranging from 1500 °C to 1650 °C with 50 °C intervals and one hour soaking time at the maximum firing temperature. Heating and cooling rates were 5 °C/min.

### (2) Characterization

The densification parameters of the fired samples in terms of bulk density and apparent porosity were evaluated with the liquid displacement method (ASTM C-20). The different phases in the powdered samples developed during firing were identified by means of X-ray diffraction analysis (XRD) with a Philips X-ray diffractometer, model PW 1730, with a Cu target and Ni filter. The XRD patterns were obtained at room temperature with goniometric range of 5–80° 2 $\theta$ , a scanning rate of 0.005°·s<sup>-1</sup> and a step size of 0.02°. The microstructure of the fractured surfaces of the as-sintered specimens was examined with a scanning electron microscope (SEM-Jeol JSM-T20). The samples were thermally etched at 1000 °C for 1 h in air atmosphere and coated with gold (thickness 15 nm) by means of electro-deposition in order to impart electric conduction. The Vickers hardness of the sintered samples was measured with a hardness tester (Omnimet automatic MHK system Model Micro Met 5114, Buehler USA). The composite samples were polished down to 0.25- $\mu$ m surface finish with diamond paste and thermally etched at 1000 °C for 1 h in air atmosphere. Indentations were made on the polished surfaces with a load of 10 kg and 15 s dwell time. 30 indents were made for each sample and the average hardness was calculated according to the following equation<sup>16</sup>:

$$H = 1.8544(P/d^2)$$

where  $p$  is the load and  $d$  is the length of the impression diagonal.

Bending strength was measured in a three-point bending test on a universal testing machine (Model LLOYD LRX5K of capacity 5kN) at a crosshead speed of 1 mm/min, and support distance of 25 mm. At least 10 specimens were measured for each data point. The fracture toughness was determined with the single-edge v-notched beam (SEVNB) technique<sup>17</sup>. For the SEVNB method, ground and polished rectangular specimens (3 x 4 x 45 mm<sup>3</sup>) were notched on the surface (3 x 45 mm<sup>2</sup>) using a diamond-charged cutting wheel, perpendicular to the length of the rectangular bars. The depth of the notches was approximately 0.7 mm, i.e.  $\leq 20$  % of the height of the specimen in accordance with DIN 51109<sup>18</sup>. The fracture toughness was determined with the following equation<sup>19</sup>:

$$K_{1c} = [L_{\max}/t(h^{1/2})] \times [L_0 - L_i/h] \times [3R_M(d/h)^{1/2}/2(1d/h)^{3/2}]$$

where  $L_{\max}$  is the maximum load,  $L_0$  and  $L_i$  are the outer and inner roller spans; respectively,  $t$  and  $h$  are thickness and height of the specimen,  $d$  is the depth of the sharpened notch.

$$R_M = [1.9887 - 1.326(d/h) - [3.49 - 0.68(d/h) + 1.35(d/h)^2](d/h)(1-(d/h))/(1+(d/h))^2]$$

### III. Results and Discussion

#### (1) Physical properties and phase composition

Fig. 1 shows the effect of the sintering temperature on the bulk density and apparent porosity of the bodies tested (X0 = pure alumina, X1 = Al<sub>2</sub>O<sub>3</sub>-0.25 wt% Nb<sub>2</sub>O<sub>5</sub>, X2 = Al<sub>2</sub>O<sub>3</sub>-0.5 wt% Nb<sub>2</sub>O<sub>5</sub>, X3 = Al<sub>2</sub>O<sub>3</sub>-0.75 wt% Nb<sub>2</sub>O<sub>5</sub>). The figure indicates that there is a positive correlation between the Nb<sub>2</sub>O<sub>5</sub> content and the bulk density of the doped alumina bodies. The increase in the Nb<sub>2</sub>O<sub>5</sub> content increases the body's bulk density and decreases its apparent porosity. It was also observed that the increase in the firing temperature increases the bulk density of the doped alumina bodies and decreases their apparent porosity. The above-mentioned results are contrary to the results obtained by Fang *et al.*<sup>20</sup> and Wang *et al.*<sup>21</sup>, which showed that doping of alumina with Y<sub>2</sub>O<sub>3</sub>, La<sub>2</sub>O<sub>3</sub> and Nd<sub>2</sub>O<sub>3</sub> retarded the densification kinetics relative to undoped alumina. They reported that the reduction in the densification rate for doped alumina can be attributed to the reduced grain boundary diffusivity. The reduction in grain boundary diffusivity is due to the segregation of dopant ions at grain boundaries to reduce the elastic strain energy that results from the difference in ionic radius between the dopants and the Al<sup>3+</sup> ion. It is postulated that the large dopant cations at the grain boundaries block the diffusion of ions along grain boundaries, leading to reduced grain boundary diffusivity. It is not the case in our study as the ionic radius of Nb<sup>5+</sup> ion is close to that of Al<sup>3+</sup> (ionic radius of Al<sup>3+</sup> and Nb<sup>5+</sup> = 0.535 and 0.69 Å respectively). We believe that the similarity of the ionic radius of Al<sup>3+</sup> and Nb<sup>5+</sup> ions facilitates the diffusion of ions along the grain boundaries and enhances the densification of the doped bodies. The increase in the Nb<sub>2</sub>O<sub>5</sub> content increases the relative density of the obtained bodies fired at 1650 °C from 91.28 % (X0) up to 98.66 % (X3), Fig. 2. Relative density was measured on the basis of the theoretical density of pure alumina, 3.97 g/cm<sup>3</sup>, and pure niobia, 4.6 g/cm<sup>3</sup>.

The XRD pattern of the as-received alumina is shown in Fig. 3. All detectable diffraction peaks correspond to those of α-Al<sub>2</sub>O<sub>3</sub>. Fig. 3 shows the XRD patterns of the fired alumina/Nb<sub>2</sub>O<sub>5</sub> bodies. The figure shows that the alumina phase is the dominant phase present. The shift in the alumina peaks indicates the formation of a solid solution between alumina and Nb<sub>2</sub>O<sub>5</sub>. The higher d values and lower 2θ shift are clearly shown in the XRD patterns of X2 and X3 samples, with 0.5 and 0.75 % Nb<sub>2</sub>O<sub>5</sub>, Fig. 3. In several studies of the binary Al<sub>2</sub>O<sub>3</sub> system<sup>22-24</sup>, Nb<sub>2</sub>O<sub>5</sub>-Al<sub>2</sub>O<sub>3</sub> compounds have been reported to occur at molar ratios of 1:1, 1:9, 1:11, 1:25 and 1:49. The most suggested binary compounds are at 1:1, 1:11, and 1:49 molar ratios. The structure of AlNbO<sub>4</sub> is built from distorted [NbO<sub>6</sub>] and [AlO<sub>6</sub>] octahedral sharing edges and corners, and linked together to give an infinite three-dimensional network<sup>24</sup>.

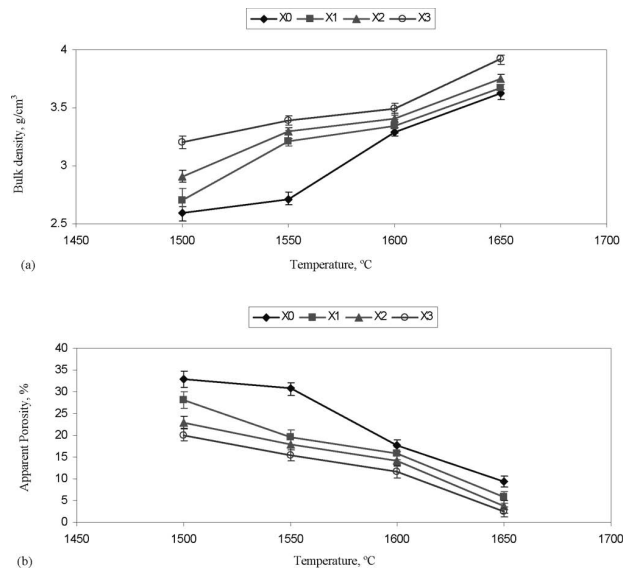


Fig. 1: Physical properties of the bodies fired at different firing temperatures, (a) Bulk density and (b) Apparent porosity.

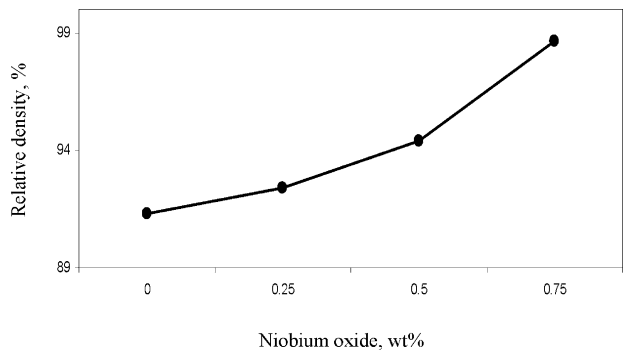


Fig. 2: Relative density of the studied bodies fired at 1650 °C.

Based on the above-mentioned results, the optimized sintering temperature seems to be 1650 °C. Accordingly, all the successive characterizations are performed for X0, X1, X2 and X3 samples sintered at 1650 °C.

#### (2) Microstructure

Figs. 4 a, b, c and d show the microstructure features of the pure alumina and alumina bodies doped with 0.25, 0.5 and 0.75 wt% Nb<sub>2</sub>O<sub>5</sub> and sintered at 1650 °C. It can be seen that the X0 sample shows abnormal growth of the alumina grains. It can be seen that alumina grains of the sample doped with 0.25 wt% Nb<sub>2</sub>O<sub>5</sub> mostly exhibit an equiaxed shape. With increased Nb<sub>2</sub>O<sub>5</sub> content, the grains tend to show abnormal grain growth. The figure shows that in contrast to the approximately uniform microstructure of the X1 sample, the grain structure of X2 and X3 samples is bimodal, comprising coarse grains (alumina having abnormal grain growth) and fine grains. The microstructure of the samples with different Nb<sub>2</sub>O<sub>5</sub> concentrations shows that some of the triple junctions are occupied by bright particles which are Nb<sub>2</sub>O<sub>5</sub>, while some other particles are present in the intragranular position within the alumina grains. In addition, Figs. 5 a and b, confirmed by EDX, proved the presence of a rare earth-alumina solid solution in the samples with 0.5 and 0.75 wt% Nb<sub>2</sub>O<sub>5</sub>, which is in complete agreement with the XRD findings.

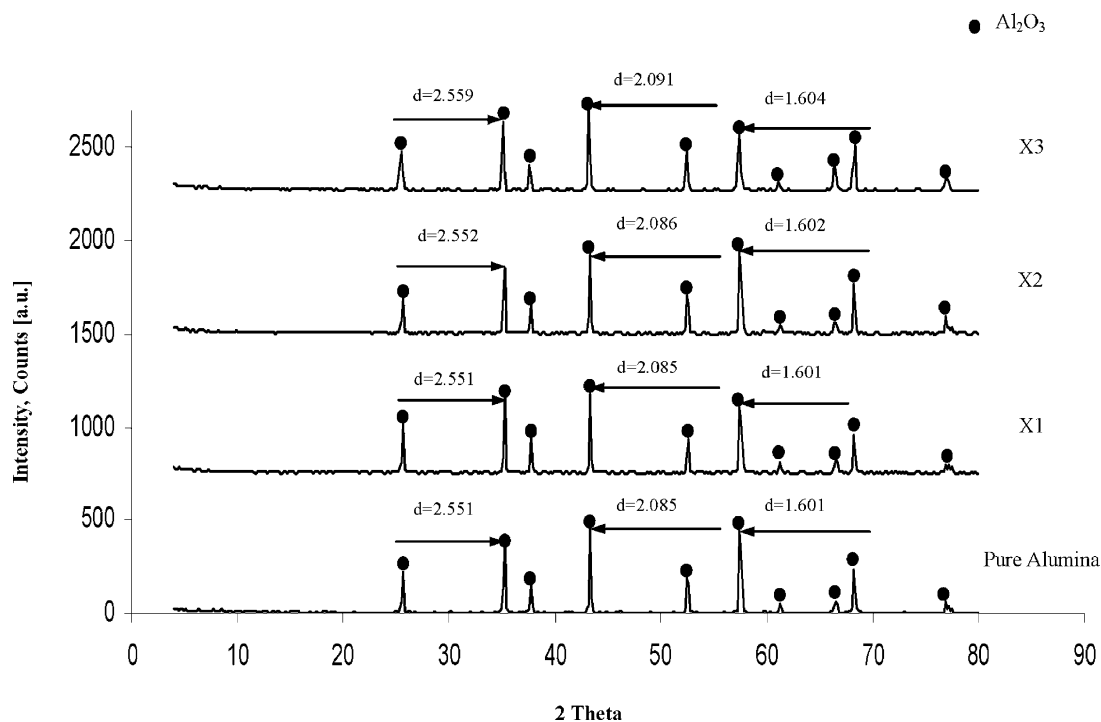


Fig. 3: XRD pattern of pure alumina, X1, X2, and X3 samples sintered at 1650 °C.

### (3) Mechanical properties

The relationship between the  $\text{Nb}_2\text{O}_5$  content of the sintered bodies and their three-point bending strength is shown in Fig. 6. The figure shows that the addition of  $\text{Nb}_2\text{O}_5$  enhanced the bending strength of the bodies. It also shows that the increase in the  $\text{Nb}_2\text{O}_5$  content increases the bending strength values. The maximum flexural strength of doped  $\text{Al}_2\text{O}_3$  ceramics is about 254 MPa when 0.75 wt%  $\text{Nb}_2\text{O}_5$  is added, which is about 34.3 % higher than that of the corresponding undoped alumina studied (189 MPa). The increase in the bending strength with the increase in  $\text{Nb}_2\text{O}_5$  content is mainly due to the increase in the densification rate and the decrease of the bodies' apparent porosity. The reason for this phenomenon was explained by Yang *et al.*<sup>5</sup> They stated that pores and microcracks had significant effects on the flexural strength of ceramics. In addition, Xihua *et al.*<sup>3</sup> note that the flexural strength of materials decreases with an increase in the materials' porosity. Therefore, the flexural strength of the studied ceramics was proportional to their bulk relative density.

Figs. 7 and 8 show the fracture toughness and Vickers hardness of pure alumina and alumina-doped  $\text{Nb}_2\text{O}_5$  bodies. The figures indicate that the increase in the  $\text{Nb}_2\text{O}_5$  content increases both the fracture toughness and hardness of the samples. The doped bodies showed remarkable improvement in both toughness and hardness at all  $\text{Nb}_2\text{O}_5$  concentrations compared to the pure alumina samples. It was noted that the improvement in the Vickers hardness is attributed to the addition of dopants, as it can improve not only the relative density but also the cohesion

between grains of alumina. Moreover, this dopant could purify and strengthen the phase interfaces and/or the grain boundaries of the ceramic matrix<sup>5,25</sup>. Also, the formation of anisotropic grains (Figs. 4 and 5) can enhance both the fracture toughness and hardness of alumina-doped bodies. Riu *et al.*<sup>26</sup> stated that the fracture toughness of ceramic materials, including  $\text{Al}_2\text{O}_3$ , increases when large elongated grains are randomly dispersed in the matrix. During the fracture process, these large grains effectively resist crack propagation in a similar way to whiskers or platelets in composite materials.

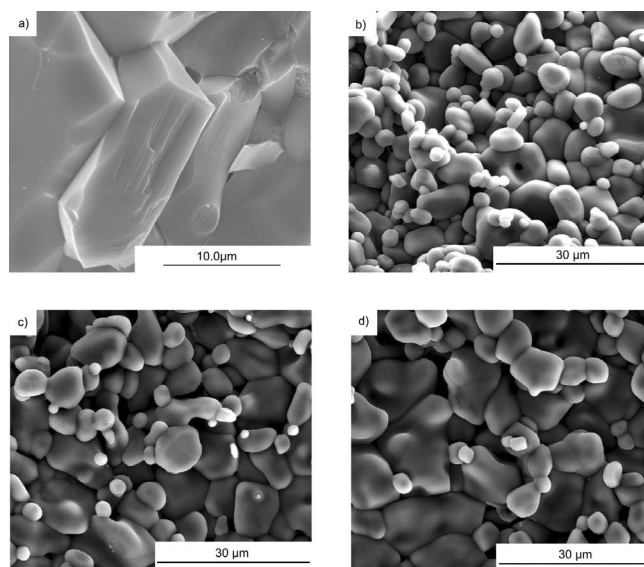


Fig. 4: SEM micrograph of X0 (a), X1 (b), X2 (c) and X3 (d) samples fired at 1650 °C.

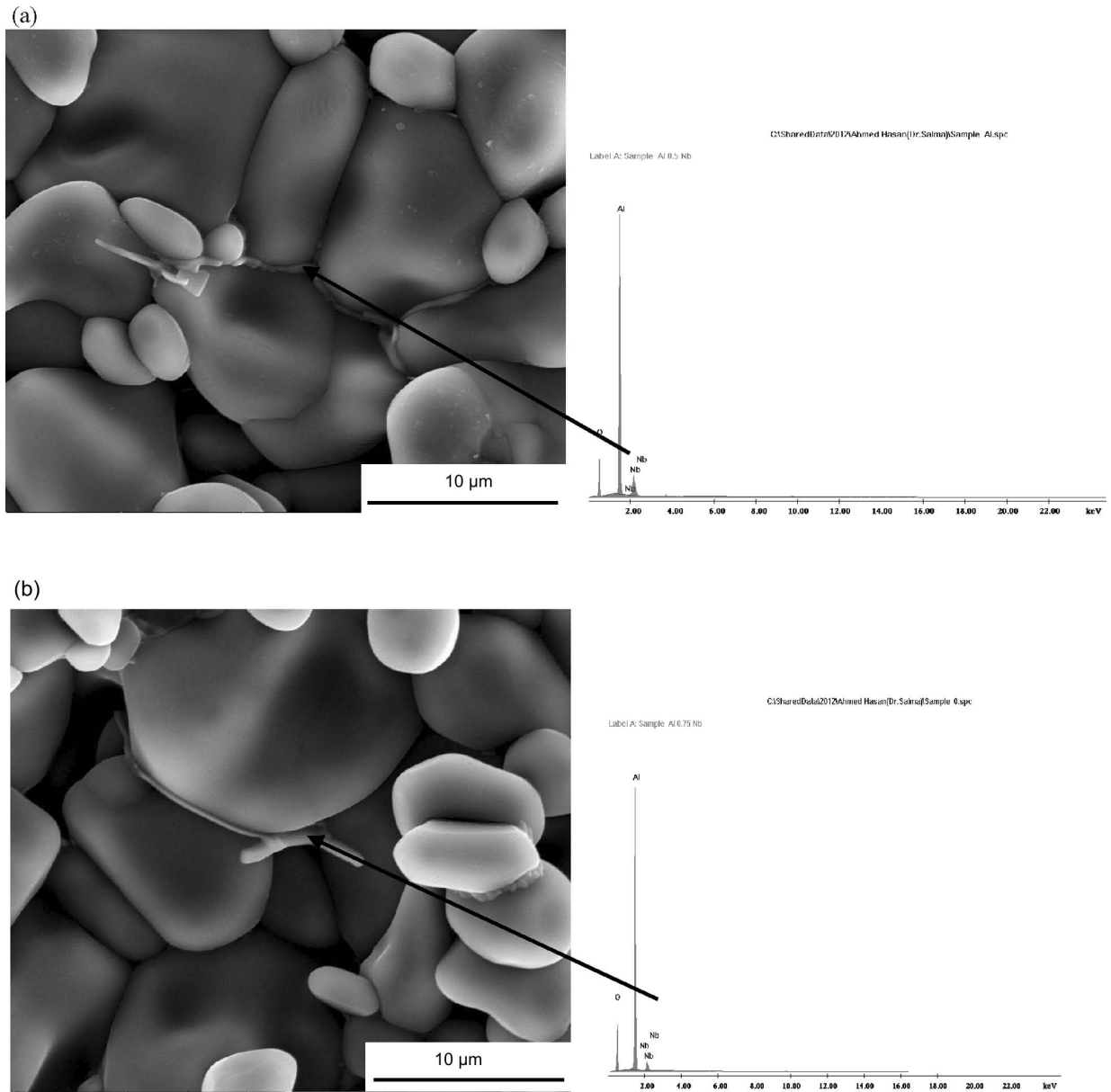


Fig. 5: SEM micrograph and EDX spectra of X2 (a) and X3 (b) samples fired at 1650 °C.

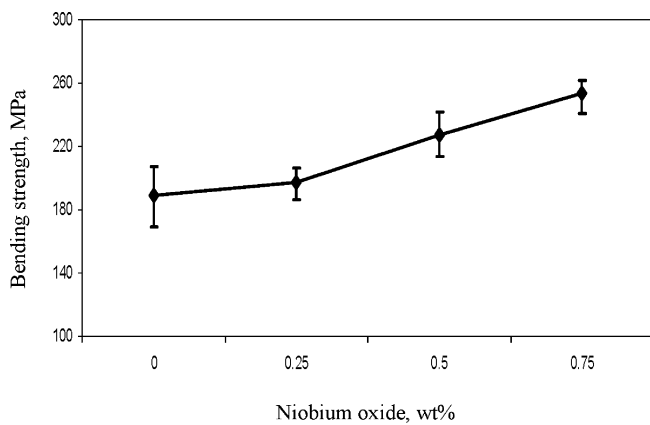


Fig. 6: Effect of Nb<sub>2</sub>O<sub>5</sub> content on the bending strength of composites sintered at 1650 °C.

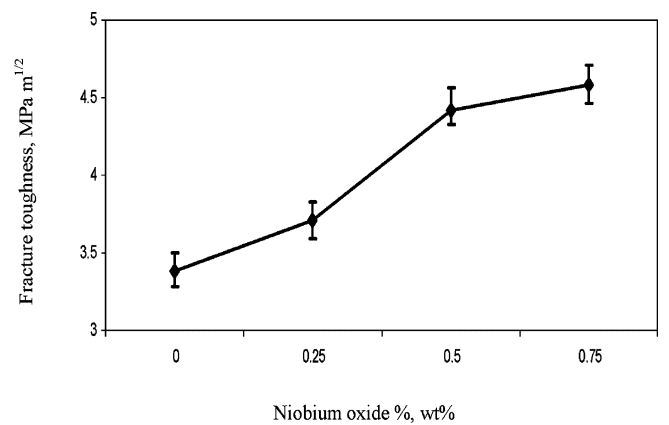


Fig. 7: Effect of Nb<sub>2</sub>O<sub>5</sub> content on the fracture toughness of composites sintered at 1650 °C.



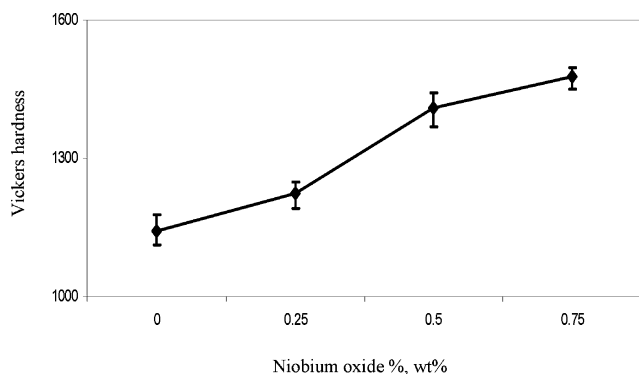


Fig. 8: Effect of  $\text{Nb}_2\text{O}_5$  content on the Vickers Hardness of composites sintered at  $1650^\circ\text{C}$ .

#### IV. Conclusions

1. Doping of alumina with  $\text{Nb}_2\text{O}_5$  enhanced the densification behavior of the alumina bodies. Bodies containing 0.75 wt%  $\text{Nb}_2\text{O}_5$  exhibited the best results.
2. Even with a small content of niobium oxide, the bending strength, hardness and fracture toughness of alumina matrix ceramic bodies were all notably improved. The maximum flexural strength, fracture toughness and Vickers hardness of the doped-alumina-based ceramics were 34.4, 35.5 and 29.5 % higher than that of the undoped ceramics.
3. The presence of  $\text{Nb}_2\text{O}_5$  was observed at the triple junctions and the intergranular regions of the  $\text{Al}_2\text{O}_3$  grains.
4. Increasing the  $\text{Nb}_2\text{O}_5$  content led to the formation of a rare-earth-containing liquid phase in the samples. The presence of such phase proves its decisive role in the abnormal grain growth in the  $\text{Al}_2\text{O}_3$ .

#### References

- 1 Maiti, K., Sil, A.: Microstructural relationship with fracture toughness of undoped and rare earths (Y, La) doped  $\text{Al}_2\text{O}_3$ - $\text{ZrO}_2$  ceramic composites, *Ceram. Int.*, **37**, 2411–2421, (2011).
- 2 Oungkulsomkongkol, T., Salee-Art, P., Buggakupta, W.: Hardness and fracture toughness of alumina-based particulate composites with zirconia and strontia additives, *J. Met. Mat. & Min.*, **20**, [2], 71–78, (2010).
- 3 Xihua, Z., Changxia, L., Musen, L., Jianhua, Z.: Research on toughening mechanisms of alumina matrix ceramic composite materials improved by rare earth additive, *J. Rare Earths*, **26**, [3] 367–370, (2008).
- 4 Zhang, X.H., Liu, C.X., Li, M.S., Zhang, J.H., Sun, J.L.: Toughening mechanism of alumina-matrix ceramic composites with the addition of  $\text{AlTiC}$  master alloys and  $\text{ZrO}_2$ , *Ceram. Int.*, **35**, 93–97, (2009).
- 5 Yang, Y., Wang, Y., Tian, W., Wang, Z., Zhao, Y., Wang, L., Bian, H.: Reinforcing and toughening alumina/titania ceramic composites with nano-dopants from nanostructured composite powders, *Mat. Sci. & Eng. A*, **508**, 161–166, (2009).
- 6 Rani, D.A., Yoshizawa, Y., Hirao, K., Yamauchi, Y.: Effect of rare-earth dopants on mechanical properties of alumina, *J. Am. Ceram. Soc.*, **87**, [2], 289–292, (2004).
- 7 Galmarini, S., Aschauer, U., Tewari, A., Aman, Y., Van Gestel, C., Bowen, P.: Atomistic modeling of dopant segregation in  $\alpha$ -alumina ceramics: coverage dependent energy of segregation and nominal dopant solubility, *J. Eur. Ceram. Soc.*, **31**, 2829–2852, (2011).
- 8 West, G.D., Perkins, J.M., Lewis, M.H.: The effect of rare earth dopants on grain boundary cohesion in alumina, *J. Eur. Ceram. Soc.*, **27**, 1913–1918, (2007).
- 9 French, J.D.: High temperature deformation and fracture toughness of duplex ceramic microstructures, Ph.D. Thesis Lehigh University, Bethlehem, PA, (1993).
- 10 Przybylski, K., Garratt-Reed, A.J., Pint, B.A., Katz, E.P., Yurek, G.J.: Segregation of Y to grain boundaries in the  $\text{Al}_2\text{O}_3$  scale formed on a ODS alloy, *J. Electrochem. Soc.*, **143**, 3207–3208, (1987).
- 11 Gruffel, P., Carry, C.: Effect of grain size on yttrium grain boundary segregation in fine-grained alumina, *J. Eur. Ceram. Soc.*, **11**, 189–199, (1993).
- 12 Deng, Z.Y., Zhou, Y., Brito, M.F., Tanaka, Y., Ohji, T.: Effects of rare earth dopants on grain boundary bonding in alumina-silicon carbide composite, *J. Eur. Ceram. Soc.*, **24**, 511–516, (2004).
- 13 Acchar, W., Segades, A.M.: Properties of sintered alumina reinforced with niobium carbide critical, *Int. J. of Ref. Met. & Hard Mat.*, **27**, 427–430, (2009).
- 14 Zhao, G., Huang, C., Liu, H., Zou, H., Zhu, H., Wang, J.: Preparation of in-situ growth TaC whiskers toughening  $\text{Al}_2\text{O}_3$  ceramic matrix composite, *Int. J. of Ref. Met. & Hard Mat.*, **36**, 122–125, (2013).
- 15 Chan, H.M., Harmer, M.R.: Effect of  $\text{Nb}_2\text{O}_5$  doping on the densification and abnormal grain growth behavior of high-purity alumina, *J. Am. Ceram. Soc.*, **87**, [3], 378–383, (2004).
- 16 Anstis, G.R., Chantikul, P., Lawn, B.R., Marshall, D.B.: A critical evaluation of indentation techniques for measuring fracture toughness: I, Direct crack measurement, *J. Am. Ceram. Soc.*, **64**, 533–538, (1981).
- 17 Tang, D., Lim, H., Lee, K., Lee, C., Cho, W.: Evaluation of mechanical reliability of zirconia-toughened alumina composites for dental implants, *Ceram. Int.*, **38**, 2429–2436, (2012).
- 18 Prüfung von keramischen Hochleistungswerkstoffen, Ermittlung der Risszähigkeit  $K_{Ic}$  (Testing high-performance ceramic materials, determination of the fracture toughness,  $K_{Ic}$ , in German), Berlin, Beuth-Verlag, (1991).
- 19 Munz, D., Fett, T.: Ceramics: mechanical properties, failure behaviour, materials selection, Berlin, Springer-Verlag, (1999).
- 20 Fang, J., Thompson, A.M., Harmer, M.P., Chan, H.M.: Effect of yttrium and lanthanum on the final-stage sintering behavior of ultrahigh-purity alumina, *J. Am. Ceram. Soc.*, **80**, [8], (1997), 2005–2012.
- 21 Wang, C-M., Chan, H.M., Harmer, M.P.: Effect of  $\text{Nd}_2\text{O}_3$  doping on the densification and abnormal grain growth behavior of high-purity alumina, *J. Am. Ceram. Soc.*, **87**, [3], (2004), 378–383.
- 22 Yamaguchi, O., Tomihisa, D., Shimizu, K.: Formation and transformation of  $\delta$ - $\text{Nb}_2\text{O}_5$  solid solutions in the system  $\text{Nb}_2\text{O}_5$ - $\text{Al}_2\text{O}_3$ , *Z. Anorg. Allg. Chem.*, **569**, 177–182, (1989).
- 23 Muller, E.K., Nicholson, B.J.: Concerning the phase diagram and dielectric behavior of the oxide system  $\text{Al}_2\text{O}_3$ - $\text{Nb}_2\text{O}_5$ , *J. Am. Ceram. Soc.*, **45**, [5], 250–251, (1962).
- 24 Pedersen, B.F.: The crystal structure of aluminum niobium oxide ( $\text{AlNbO}_4$ ), *Acta. Chem. Scand.*, **16**, 421–430, (1962).
- 25 Chonghai, X., Chuanzhen, H., Xing, A.: Toughening and strengthening of advanced ceramics with rare earth additives, *Ceram. Int.*, **32**, 423–429, (2006).
- 26 Riu, D., Min Kong, Y., Kim, H. E.: Effect of  $\text{Cr}_2\text{O}_3$  addition on microstructural evolution and mechanical properties of  $\text{Al}_2\text{O}_3$ , *J. Eur. Ceram. Soc.*, **20**, 1475–1481, (2000).